Int. J. Simul. Multisci. Des. Optim. 2014, **5**, A14
© S. Messai et al., Published by EDP Sciences, 2014
DOI: 10.1051/smdo/2013018

IJSMDO

Available online at:
www.ijsmdo.org

ARTICLE OPEN ACCESS

Comparison of 1D and 2D models predicting a packed bed drying

Souad Messai[1,*], Mohamed El Ganaoui[2], Jalila Sghaier[3], Laurent Chrusciel[2], and Slimane Gabsi[1]

[1] Unité de Recherche Environnement, Catalyse et Analyse des Procédés URECAP, Ecole Nationale d'Ingénieurs de Gabès, Rue Omar Ibn-Elkhattab, 6029 Gabès, Tunisie
[2] Laboratoire d'Etudes et de Recherche sur le Matériau Bois LERMAB, Université de Lorraine-Faculté des Sciences et Technologies, Boulevard des Aiguillettes, 54506 Vandœuvre-lès-Nancy Cedex, France
[3] Laboratoire d'Energétique et des Transferts Thermiques et Massiques, Faculté des Sciences de Tunis, Campus Universitaire, 2092 El Manar, Tunisie

Received 10 July 2013 / Accepted 13 November 2013 / Published online 10 February 2014

Abstract – A numerical study for the modelling of porous particles packed bed drying in one and two dimensions (1D and 2D) is presented in this work. This model is based on the averaging volume approach using two scale changes. Taking into account the non validity of the thermal equilibrium between the gas phase and the porous particle, a two temperatures model is then developed. The numerical resolution of macroscopic equations describing heat and mass transfer during the drying of a packed bed is carried out by the method of finite volume. Experimental data for spherical porous alumina particles reported in the literature were used for the validation of the model. A good agreement was found. The influence of particles thermophysical properties and operating variables is tested. A set of time-space evolution describes the progression of these variables with time, in the height and radius of the packed bed. The model results allow a better understanding of the heat and mass transfer mechanisms involved in a packed bed drying process.

Key words: Superheated steam, Drying, Averaging volume, 1D and 2D model, Porous media.

Nomenclature

A	Specific surface, m^2/m^3
Cp_g	Gas specific heat, J kg^{-1} K^{-1}
Cp_S	Solid specific heat, J kg^{-1} K^{-1}
d	Particle diameter, m
F_m	Mass flux, kg $m^{-2}s^{-1}$
H	Height of the packed bed, m
h_{sg}	Convective heat transfer coefficient at solid-gas interface, W m^{-2} K^{-1}
h_0	Heat transfer coefficient at the inlet of the bed, W m^{-2} K^{-1}
h_1	Heat transfer coefficient at the outlet of the bed, W m^{-2} K^{-1}
$\dot{m}$	Evaporation rate (mass flow rate of water vapor per m^3 of drying gas) kg m^{-3} s^{-1}
m_g	Gas mass flux, kg m^{-2} s^{-1}
$\boldsymbol{n}$	Unit normal vector
$\boldsymbol{n}_{gs}$	Unit normal vector at the solid-gas interface
P	Pressure, Pa
t	Time, s
T	Temperature, K
R	Radius of the bed, m
X	Absolute moisture content kg of water/kg of dry mass
V_g	Gas velocity, m s^{-1}
Z	Axial coordinate, m

Greek symbols

L_v	Latent heat of vaporization, J kg^{-1}
ρ	Density, kg m^{-3}
μ	Dynamic viscosity, Pa s
λ	Thermal conductivity, W m^{-1} K^{-1}
ε	Porosity

Subscripts

eff	Effective
g	Gas phase
s	Solid phase
sg	Solid gas interface
l	Liquid phase
v	Vapor phase

Superscripts

g	Gas
s	Solid
l	Liquid

*Corresponding author: souad.messai@gmail.com

Introduction

Solid-fluid contact technique is widely applied in agriculture and chemical engineering in the form of packed bed drying. Indeed, modeling simultaneous heat and mass transfer occurring between the particles and the drying medium during the circulation through the packed bed, is complex. Because of its great technological applications, packed bed drying has been studied for many years. In fact, one of the first models for packed bed dryers, the one-phase model proposed by Thompson [1] was significant at that time for dryer design. Currently, a large variety of models has been developed for describing the heat and mass transfer inside packed bed dryers. Riede and Schlünder [2] described the mass transfer in a single particle with a modified shrinking core model for drying of fixed beds. Many assumptions are used to simplify the equations describing the transport mechanisms. Saastamoinen and Impola [3] developed a fixed bed drying model for the description of heat and mass transfer in a single particle considering the capillary pressure effects. Khan et al. [4] incorporated a front particle model into the modeling of a packed bed of alumina porous particles during superheated steam drying. This model has been validated with their experimental results. They assumed that capillary action had no effect on moisture transfer in the material and the drying process was controlled by internal heat transfer. In the similar way, Hager et al. [5] studied numerically and experimentally the steam drying process of a bed of porous particles (ceramic and alumina). The process is analyzed in terms of the hybrid model, that apply the volume averaged transport equation for the fluid flowing in the fixed bed and the local equations for heat and mass transfer taking place in the particle. Chen et al. [6] integrated a single particle model with a two-phase hydrodynamic to simulate the drying of coal in a fluidized bed with superheated steam.

Other studies investigated fixed bed steam drying of foodstuff by dividing the bed in three zones (dry zone, drying zone and wet zone) limited by two interfaces [7]. A dry front separates the dry zones from the ones and a wet front partition the drying and wet zones. The moisture content and temperature of the dry zone are equal to their equilibrium moisture content and steam temperature, respectively.

On other way, many researchers have developed mathematical models for humid air drying especially for low and average temperature. Arnaud and Fohr [8] proposed a partial differential equations model for the slow drying of a deep bed at low temperature. They proved the existence of a drying front which moves in the granular media without distortions. Sözen and Vafai [9] studied the transient forced convective condensing gas flux through a packed bed. The non validity of local thermal equilibrium assumption between the solid and fluid phases is assumed. They examined two different types of boundary conditions. The condensation in vapor phase has been also studied. Mhimid et al. [10] presented a two temperatures 2D-model for the drying of a cylindrical and granular bed with imposed hot air flux and conductive heat flux at the wall. The time-space evolution of temperature has been also studied. Ratti and Mujumdar [11] developed a model to simulate batch drying. They studied numerically the effect of airflow reversal for the batch drying of foodstuff in a deep bed. Wang and Chen [12] proposed a model of fixed bed drying of moist porous particles. They considered the distribution effects of moisture content, temperature and gas pressure of the particle and the conjugate effect between gas and particles. They divided the bed into series of thin layers. Kato et al. [13] studied a packed bed dryer using air as drying agent and developed a model of packed bed drying. With combination of heat transfer data, they predicted the drying process of activated alumina.

Otherwise modeling of heat and mass transfer in 1D and 2D configuration is also available in the literature. Izadifar et al. [14] presented a 1D-model for packed bed drying using the local volume averaging (LVA) approach, with local thermal equilibrium in each elementary volume in order to derive transient heat and mass transfer equations, solved by means of an implicit numerical method. Stakić et al. [15] developed a 1D-model for the case of convective drying of hygroscopic material in a packed bed. The assumption of local thermal equilibrium is assumed. The drying rate of the specific product is calculated by applying the concept of a drying coefficient, called a global mass transfer and often used to characterize mass transfer in chemical processes. Zili and Ben Nasrallah [16] developed a 2D-model to simulate forced convection air drying of granular products at low and average temperatures. The authors presented a general model taking into account conduction, convection and diffusion using variable coefficients. The assumption of local thermal equilibrium is not assumed. They demonstrated the effect of variable porosity and intermittent flux on the drying process. Recent models by Sitompul et al. [17] and Istadi and Sitompul [18] developed a 2D-model for spherical grains deep-bed drying taking into account transport phenomena within the bed. Moreover, the effect of air velocity distribution (pressure field) on the drying process was studied. Mainly the same model [19] was used for a different dryer geometry (large diameter column). Boukadida et al. [20] developed a 2D model to investigate heat and mass transfer during convective drying of clay brick. The effect of gaseous pressure is taken into account. The authors studied the effect of drying agent properties on drying kinetics and space-time evolution of drying parameters.

In this work, we developed a 2D-model describing heat and mass transfer during drying of a packed bed in superheated steam. The important advantages of superheated steam drying that are of interest to industries include the absence of oxidative reactions due to the absence of oxygen and high drying rates in both constant and falling rate periods [21–24].

The mathematical model is developed using two change of scale. Convective heat transfer is assumed between the granular bed and steam. To take into account the thermal non-equilibrium between the porous and the fluid phases a two-temperature macroscopic model is used to describe heat transfer. The mass transfer is introduced in the form of drying kinetics deduced from a single particle model. The predicted results from the packed bed model from the 1D and 2D models were compared to the experimental data in the literature. The comparison of time-space evolution of drying parameters shows the existence of drying front for 2D model.

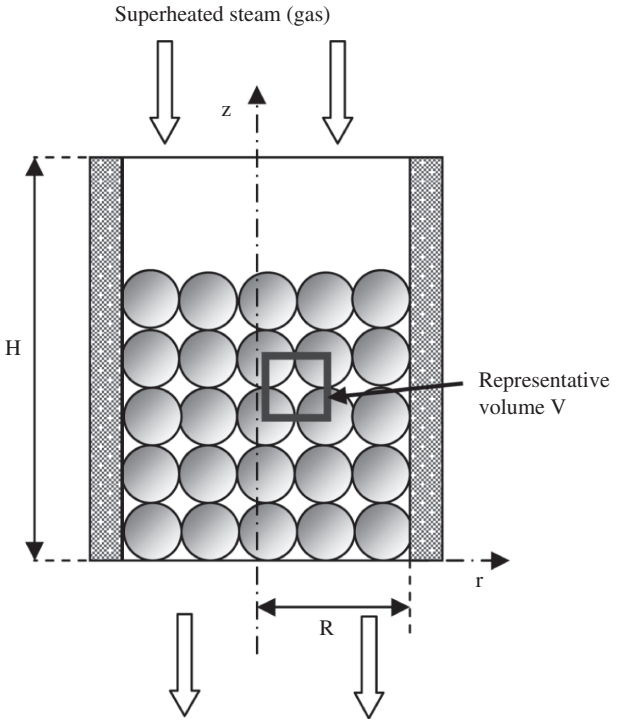

Figure 1. Geometrical configuration of the fixed bed and averaging volume of the bed.

Mathematical model

Knowledge of the heat transfer characteristics and spatial temperature distribution in packed beds is of great importance to the design and analysis of the packed beds dryers. Hence, an attempt is made to develop a model based on the averaging approach tacking into account the non validity of the thermal equilibrium. The packed bed is made of an inert and rigid solid matrix phase (spherical porous particles) and a gaseous phase (drying agent). Thus, the bed is a discontinuous medium. The theoretical formulation of heat and mass transfer in the packed bed is obtained by a change of scale [25–28]. At microscopic scale, the size of the representative volume V is small with respect to the pore sizes (Figure 1). At macroscopic scale the size of the representative volume is large with respect to the pore sizes. The change of scale allows converting the real discontinuous medium to an equivalent fictional continuous one.

Governing equations of heat and mass transfer

The macroscopic differential equations are obtained by taking the average of the microscopic equations over the averaging volume and using closing assumptions. Several simplifying assumptions are made in order to obtain a closed set of macroscopic governing equations:

- the porous medium is from a macroscopic point of view homogeneous and isotropic,
- non validity of the thermal equilibrium,
- the bed porosity is uniform in all the directions,
- the compression work and viscous dissipation are negligible,
- the dispersion and tortuosity terms are modeled as diffusion fluxes,

For an arbitrary α-phase scalar or tensor variable ψ_α, we note:

Superficial average:

$$\langle \psi_\alpha \rangle = \frac{1}{v} \int_{v_\alpha(t)} \psi_\alpha \mathrm{d}v. \tag{1}$$

Intrinsic average:

$$\langle \psi_\alpha \rangle^\alpha = \frac{1}{v_\alpha(t)} \int_{v_\alpha(t)} \psi_\alpha \mathrm{d}v. \tag{2}$$

The superficial and intrinsic average are related by:

$$\langle \psi_\alpha \rangle = \varepsilon_\alpha \langle \psi_\alpha \rangle^\alpha, \tag{3}$$

where $\varepsilon_\alpha = V_\alpha / V$ is the α-phase volume fraction or porosity.

The macroscopic equations governing heat and mass transfers in the packed bed are:

Energy conservation equation in the gas phase:

$$\begin{aligned} &C_{pg}\varepsilon \langle \rho_g \rangle^g \frac{\partial \langle T_g \rangle^g}{\partial t} + \langle \rho_g \rangle^g \langle V_g \rangle C_{pg} \nabla \langle T_g \rangle^g \\ &= \nabla \cdot \left[\lambda_{\mathrm{geff}} \nabla \langle T_g \rangle^g \right] - \dot{m} C_{pg} \left(\langle T_g \rangle^g - \langle T_s \rangle^s \right) \\ &\quad - h_{gs} A \left(\langle T_g \rangle^g - \langle T_s \rangle^s \right). \end{aligned} \tag{4}$$

Energy conservation equation in the solid phase s:

$$\begin{aligned} (1-\varepsilon) C_{ps} \langle \rho_s \rangle^s \frac{\partial \langle T_s \rangle^s}{\partial t} &= \nabla . (\lambda_{\mathrm{seff}} \nabla \langle T_s \rangle^s) - \dot{m} L_v \\ &\quad + h_{gs} A \left(\langle T_g \rangle^g - \langle T_s \rangle^s \right), \end{aligned} \tag{5}$$

$\dot{m}$ is the evaporation rate defined as: $\dot{m} = A F_m$ A is the specific surface (defined as the ratio apparent surface of the particle divided by the apparent volume of particle), λ_{seff} and λ_{geff} are respectively the effective thermal conductivity of solid and gas phases and h_{gs} is the gas-particle convective heat transfer coefficient.

$$h_{\mathrm{gs}} = \frac{Nu \lambda_{\mathrm{geff}}}{d}, \tag{6}$$

where $Nu = 2 + 0.66 Re^{0.52} Pr^{0.33}$ [28]

Initial Conditions

Initially, temperatures and moisture contents are constant:

$$\langle T_g \rangle^g (0, r, z) = \langle T_s \rangle^s (0, r, z) = T_i, \tag{7}$$

$$X(0, r, z) = X_i. \tag{8}$$

Thermal boundary conditions

Several simplifying assumptions are made in order to obtain a closed set of macroscopic governing equations:

- The lateral surface of the bed is adiabatic.
- At the inlet of the cylinder defining the volume of the fixed bed, the temperature of the gas is assumed constant, the solid and gas temperatures are related by:

$$-\lambda_{\text{seff}}\frac{\partial\langle T_s\rangle^s}{\partial z}(t,r,0)=h_0\left(\langle T_s\rangle^s-\langle T_g\rangle^g\right). \tag{9}$$

- At the outlet of the cylinder, a heat transfer coefficient is introduced to describe the transfer:

solid phase

$$-\lambda_{\text{seff}}\frac{\partial\langle T_s\rangle^s}{\partial z}(t,r,H)=h_1\left(\langle T_s\rangle^s-\langle T_g\rangle^g\right), \tag{10}$$

h_0 and h_1 are the heat transfer coefficients at the entry of the cylinder and that of the wall to bed, respectively.

The main difference between 1D and 2D models is the boundary conditions. In fact, for the 1D model, the heat transfer coefficients at the entry of the cylinder and that of the wall to bed are null. Thus, radial transfer is not taken into account.

Dying kinetics

In a previous paper [29], mathematical model for the superheated steam drying of a single porous particle was developed and compared with experiment. The single particle model is integrated to simulate the continuous drying of a porous particles packed bed with superheated steam. Hence, the mass flux calculated from the single porous particle model is incorporated in the bed model. In fact, the phenomenon of water evaporation and mass transfer in a solid particle and the surrounding gas phase is expressed by drying kinetic. The evaporated rate $\dot{m}$ is given by:

$$-(1-\varepsilon)\langle\rho_s\rangle^s\frac{\partial X}{\partial t}=\dot{m}, \tag{11}$$

$$\dot{m}=AF_{\text{m}}. \tag{12}$$

A is the specific surface, as mentioned above F_{m} is the mass flux obtained by the numerical resolution of a single particle model [29, 30].

The correlations of mass flux are obtained from a set of numerical tests carried out for various values of temperatures and steam velocity of a single particle model. These correlations are incorporated in the bed model.

The parameters that influence the mass flux in the constant rate period are the gas temperature (T_{g}) and the gas velocity (V_{g}) [29]:

$$F_{\max}=F_{\max}\left(T_g,V_g\right). \tag{13}$$

$F_{\max}$ is the mass flux value in the constant rate period (CRP).

First, correlation of maximum mass flux and moisture content are deduced as function of steam temperature for a given steam velocity. Then, the steam temperature is constant, we vary the steam velocity. Different correlations are also obtained according to the steam velocity for a given steam temperature. Different correlation parameters are illustrated in Figure 2:

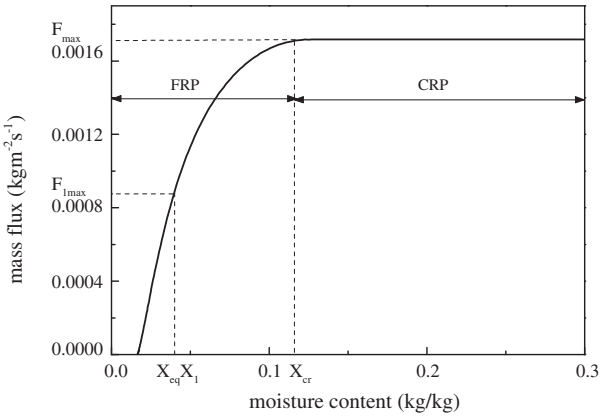

Figure 2. Different parameters of mass flux correlation.

$$F_{\max}=\frac{\left(a_1T_g-b_1\right)\ \left(c_1{V_g}^{d_1}\right)}{e_1}. \tag{14}$$

$F_{1\max}$, is the mass flux corresponding to the point of intersection of two under-periods of the falling-rate period (FRP) given by:

$$F_{1\,\max}=\frac{\left(a_2T_g-b_2\right)\ \left(c_2{V_g}^{d2}\right)}{e_2}. \tag{15}$$

The equilibrium moisture content X_{eq} is independent of steam velocity. Its expression is given according to the steam temperature:

$$X_{\text{eq}}=a_3\left(T_g\right)^{b3}. \tag{16}$$

X_{cr} the critical moisture content indicating the start of the falling-rate period is given by:

$$X_{\text{cr}}=\frac{\left(a_4T_g-b_4\right)\ \left(c_3V_g+d_3\right)}{e_3}, \tag{17}$$

X_1 is the moisture content which corresponds to the point of intersection of two under-periods of the falling-rate period:

$$X_1=\frac{\left(a_5{T_g}^{b_5}\right)\ \left(c_4V_g+d_4\right)}{e_4}, \tag{18}$$

a_i, b_i, c_i, d_i and e_i are coefficients which depend of the medium used.

The values of different constants are listed in Table 1.

Final correlations of different parameters are:

$$X>X_{\text{cr}}\longrightarrow F_{\text{m}}=F_{\max}, \tag{19}$$

$$X_1<X<X_{\text{cr}}\longrightarrow F_m=\left(F_{\max}-F_{1\,\max}\right)\left(\frac{X-X_1}{X_{\text{cr}}-X_1}\right)+F_{1\,\max}, \tag{20}$$

$$X_{\text{eq}}<X<X_1\longrightarrow F_m=F_{1\,\max}\left(\frac{X-X_{\text{eq}}}{X_1-X_{\text{eq}}}\right). \tag{21}$$

Table 1. Values of constants for drying kinetic with superheated steam.

Constants	Values
a_1	2.257×10^{-5}
a_2	8.76×10^{-6}
a_3	27.83×10^{-3}
a_4	1.92×10^{-4}
a_5	0.449×10^{2}
b_1	8.483×10^{-3}
b_2	0.3294×10^{-2}
b_3	-48.83×10^{-2}
b_4	5.381×10^{-2}
b_5	-140.9×10^{-2}
c_1	13.448×10^{-4}
c_2	0.050872×10^{-4}
c_3	6.592×10^{-3}
c_4	-1.418×10^{-3}
d_1	27.28×10^{-2}
d_2	14.14×10^{-2}
d_3	2.56×10^{-2}
d_4	1.0886×10^{-2}
e_1	10.04×10^{-4}
e_2	5×10^{-4}
e_3	30×10^{-3}
e_4	9×10^{-3}

These correlations of mass flux are integrated on the scale of the granular bed.

Numerical resolution

The system of equations is solved by a finite volume method based on the notion of a control domain [31] with a no regular mesh. To insure the convergence, an upwind scheme is used to evaluate convection terms on faces of the control domain. The discretization of the conservation equations leads to a system of algebraic equations. This system is strongly coupled and is solved numerically by the iterative method of Gauss Seidel.

Validation

The validity of the model to predict the evolution of temperature and drying rate throughout the granular bed during convective superheated steam drying is confirmed by using sets of data available for the drying of porous particles [28]. The authors investigated experimentally superheated steam drying of porous alumina and ceramic particles packed bed with a diameter of 9.5 and 10 mm, respectively. A high-resolution load cell continuously registered the weight of the entire test section, and the steam inlet and outlet temperatures were monitored as well as the centre temperature of a varying number of spheres. The internal bed vessel is a cylinder with a diameter of 0.3 m. The bed height was varied from 100 to 200 mm. All the experiments were performed at atmospheric pressure. Figures 3 and 4 illustrate the comparison of the model calculations with

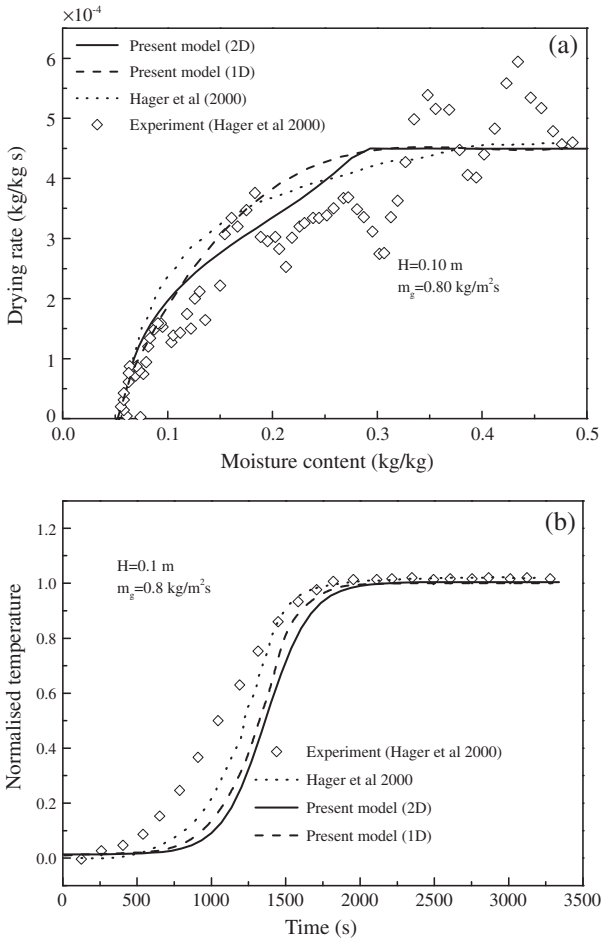

Figure 3. Comparison of experimental and numerical data of drying rate (a) and outlet steam temperature (b) of alumina particles packed bed for various operating parameters.

experimental data of the drying rate and the steam outlet temperature for varying height and steam mass flux. The curves indicate that the bed depth affects the amount of drying time. The bed having the thinnest depth (0.1 m) reaches the gas temperature and the equilibrium drying rate more quickly. Whereas, when we increase the steam mass flux for the same bed depth Reynolds number increases and consequently the convective heat transfer coefficient also increases. Thus we accelerate transfers and then the drying time decreases. As can be seen the agreement is good between predictions and experimental data, even though there is slight discrepancies that can be attributed to the position of thermocouples and errors in the measurement. Figures 3 and 4 show also the comparison of the present model in 1D and 2D configurations with the model of Hager et al. [28]. We note that there is a difference between the two models especially for the value of evaporation rate during the constant rate period. A possible explanation for discrepancies between the two models this is the approach used for communication between the particle and the packed bed. Indeed, Hager et al. [28] developed the so called hybrid model. The particle tortuosity is the only adjustable parameter. They showed that

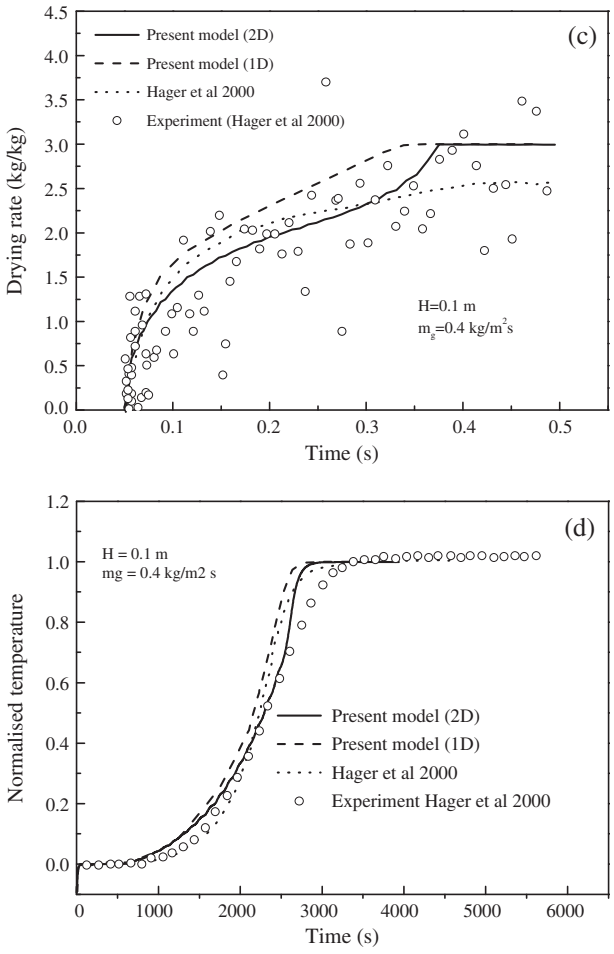

Figure 4. Comparison of experimental and numerical data of drying rate (a) and outlet steam temperature (b) of alumina particles packed bed for various operating parameters.

the variation of this parameter does not affect the drying process. The particle model is incorporated in the bed model by the temperature and the evaporation rate at the porous particle surface. The porous particle model of Hager et al. is based on the thermodynamic approach [32]. This model takes into account the effect of gravity and pressure gradient. The phenomenological coefficients involved in the transfer equations were determined experimentally or numerically. This is the disadvantage of this model since the determination of these coefficients is very complicated. Our porous particle model is based on the volume averaging approach. We used an iterative method (dichotomy) to calculate the mass flow while satisfying the boundary conditions [29, 30]. Thus, in our model, we need only physical properties of the porous medium. Experimentally, these parameters are easily accessible. The main difference between our model and that of Hager et al. is the incorporation of new correlations of mass flux and moisture content in the packed bed. These correlations are calculated from the drying of a porous particle, parameters are calculated during the constant rate period and the falling rate period.

The comparison of the 1D and 2D models shows that the 2D model fits experimental data better than the 1D model. In subsequent section, more explanation of differences between the two models is detailed.

Sensitivity analysis

Knowledge of the parameters that have significant impact on drying behavior is useful in designing drying operations. Figure 5 illustrates the effect of particle diameter on the drying process. We noted that particle diameter exerts a significant influence on the drying behavior. Larger particles require a much longer time to reach the equilibrium moisture content due to the fact that more energy is needed to heat them up. We also note that for the same drying temperatures and steam velocities, the predicted moisture content decreases much more rapidly when the diameter decreases. This is due to the fact that the Reynolds number and thus the heat transfer coefficient increases with smaller particles. As we would expect, when we increase the gas velocity, for the same drying temperature, the Reynolds number increases and consequently the convective heat transfer coefficient increases (Figure 6) leading to a reduction of the drying time. To analyze the effect of drying temperature on drying curves, we represented the evolution of the drying kinetics for four values of the gas temperature (Figure 7). As can be expected, at lower temperatures the moisture content decreases more slowly. While the temperature increases, the medium reaches the drying temperature more quickly. This is because the higher temperature gradient in the medium resulted in a higher heat flux [33].

Time-space evolution of particles temperature and moisture content

The temperature field evolution within the medium is the key to the drying phenomenon. The time-space evolution of drying parameters allows a better understanding of the heat and mass transfer mechanisms. Figure 8 shows the time-space evolution of the moisture content of the granular medium during superheated steam drying. We note the existence of a drying front which moves from the outlet to the inlet of the cylinder in the direction of fluid flow drying. This front divides the granular medium into two regions: wet and dry regions. As the drying process progresses, the dry region widens and the moisture content decreases to the equilibrium value. Indeed, an increase in the temperature of the solid during drying results in an increase of the evaporation rate which leads to a decrease in the moisture content. Figures 9 illustrates the time-space evolution of the temperature of the particle (solid phase of the packed bed) during superheated steam drying. Initially, the drying agent temperature is greater than that of the granular medium. Therefore, the temperature increases from the inlet of the cylinder ($z = H$) to the outlet ($z = 0$) and from the wall to the center, following the direction of the gas flow. Moreover the time-space evolution of temperature indicates the existence of the two classic drying periods: the constant rate period (with a level of 100 °C) and the falling rate period (when the temperature exceeds 100 °C). Drying process is achieved when moisture content and particle temperature reach the equilibrium moisture content and the drying agent temperature, respectively.

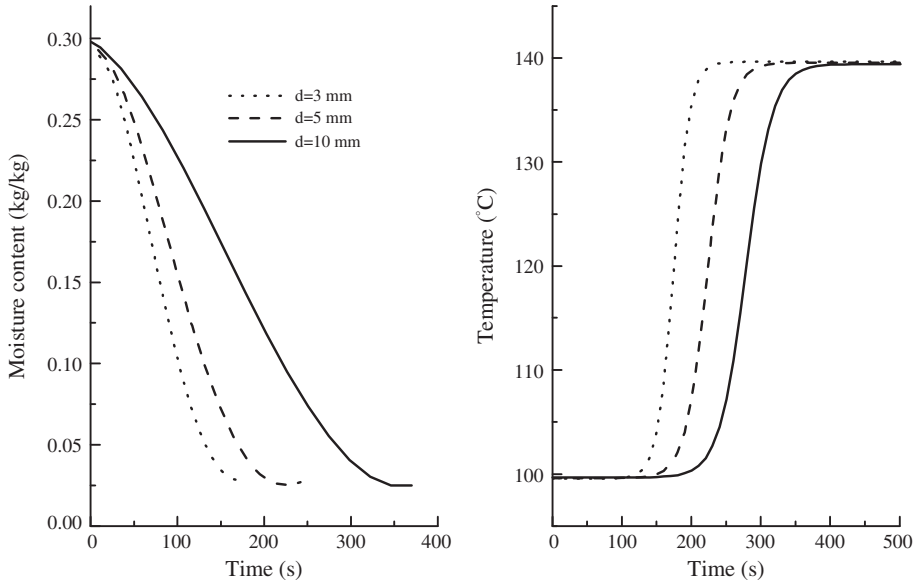

Figure 5. Effect of particle diameter on bed moisture content and temperature during superheated steam drying: V_g = 1.5 m s^{-1}, T_g = 140 °C.

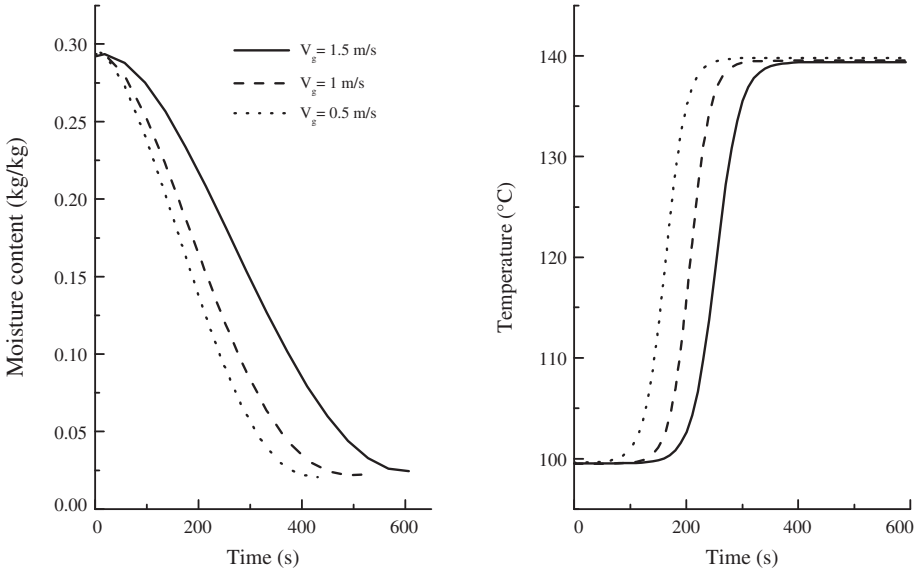

Figure 6. Effect of gas velocity on bed moisture content and temperature during superheated steam drying: d = 10 mm, T_g = 140 °C.

Comparison of 1D and 2D models

2D model is relevant in understanding real heat and mass transfer phenomena. Compared to 1D model, 2D model is used to study the transverse processes of heat and mass transfer. This model has the advantage of being more realistic, but some control mechanisms are retained. Figure 10 shows a comparison of these two models. We note from the curves of bed moisture content and temperature that the effect of taking into account 2D modeling, appears especially at the end of drying which show the influence of the internal process. Because the initial temperature is equal to that of steam saturation, the condensation phase is absent for the two models. The disadvantage of the condensation phase is the increase of the product moisture content which emphasizes the importance of preheating the product to be dried. This procedure is also used in the experimental study of Hager et al. [28]. Furthermore, the equilibrium moisture content for the 2D model is lower than that of 1D model which accentuates the importance of taking into account the lateral transfer for modeling packed bed drying. Figures 11 and 12 illustrate a comparison of the time space evolution of the moisture content and bed temperature for both models. We immediately note the existence of drying front for 2D model. The time-space evolution of 1D model shows the absence of a drying front. This is just a distribution of the moisture content and temperature within the medium. Indeed, the elevation of the

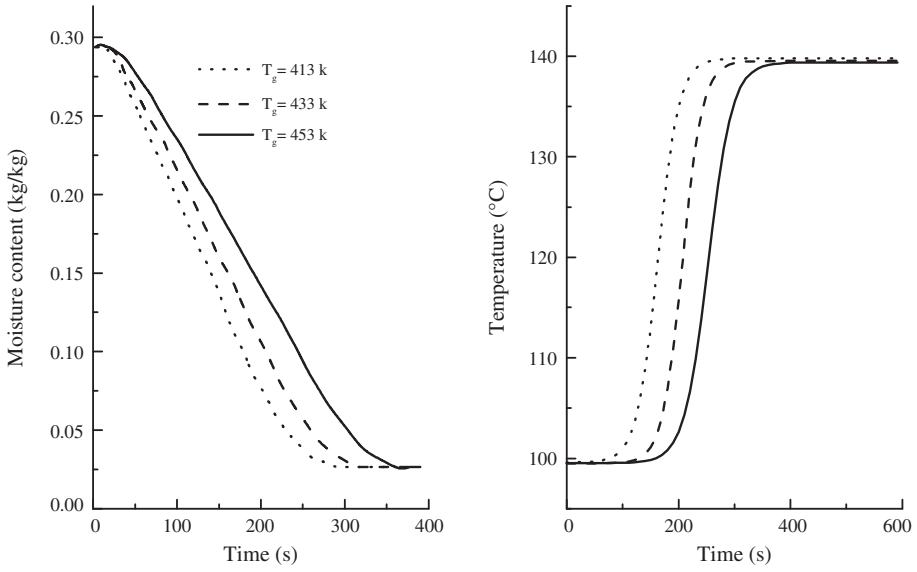

Figure 7. Effect of gas temperature on bed moisture content and temperature during superheated steam drying: d = 10 mm, V_g = 1.5 m s^{-1}

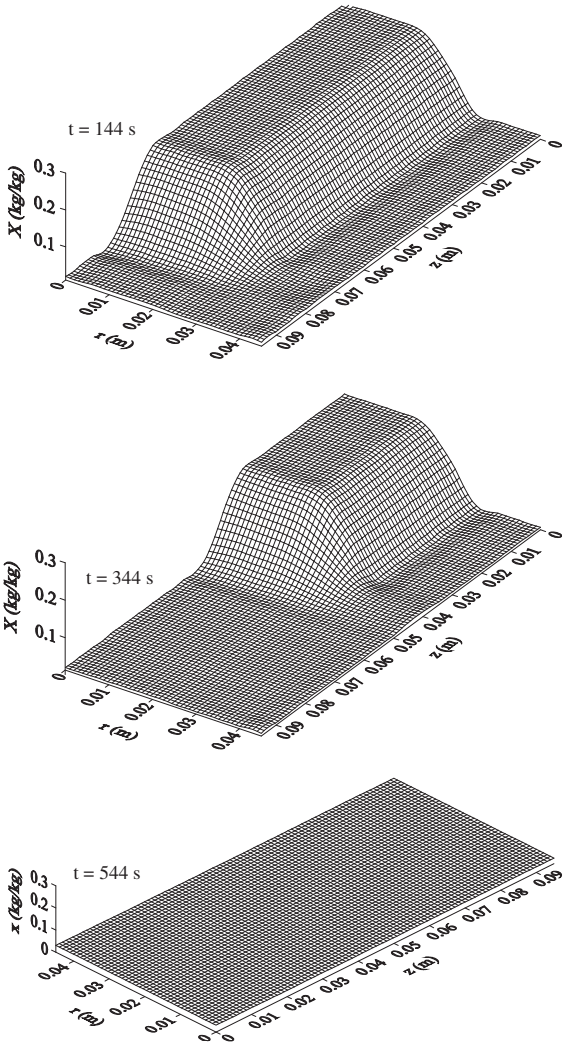

Figure 8. Time-space evolution of bed moisture content during superheated steam drying: d = 10 mm, T_g = 140 °C and V_g = 1.5 m s^{-1}.

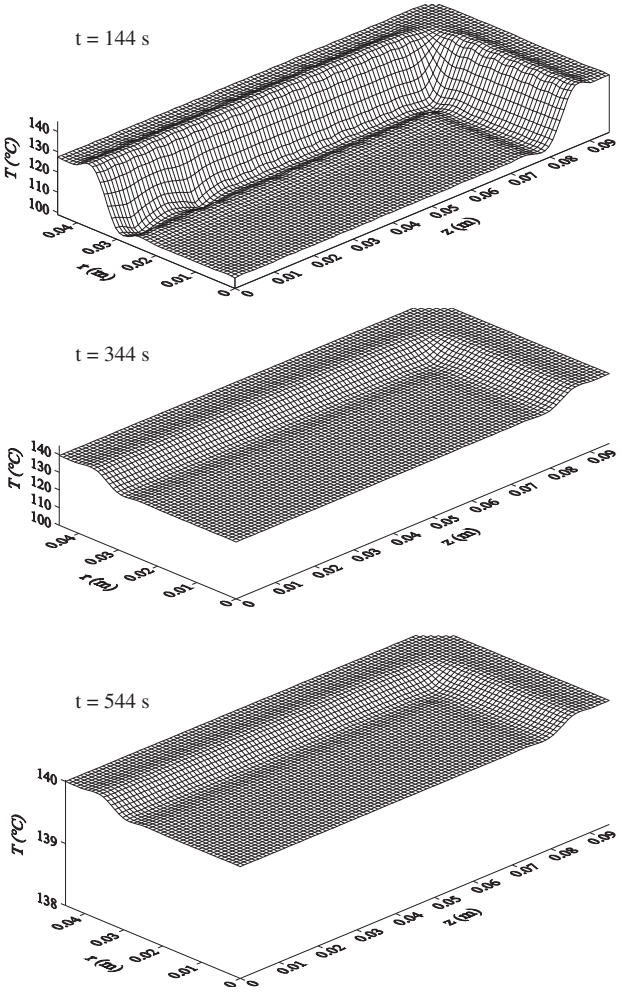

Figure 9. Time-space evolution of bed temperature during superheated steam drying: d = 10 mm, T_g = 140 °C and V_g = 1.5 m s^{-1}.

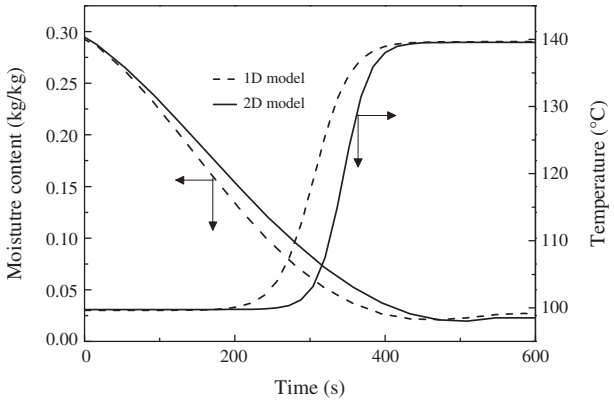

Figure 10. Comparison of moisture content and bed temperature for 1D and 2D models: d = 10 mm, T_g = 140 °C and V_g = 1.5 m s^{-1}

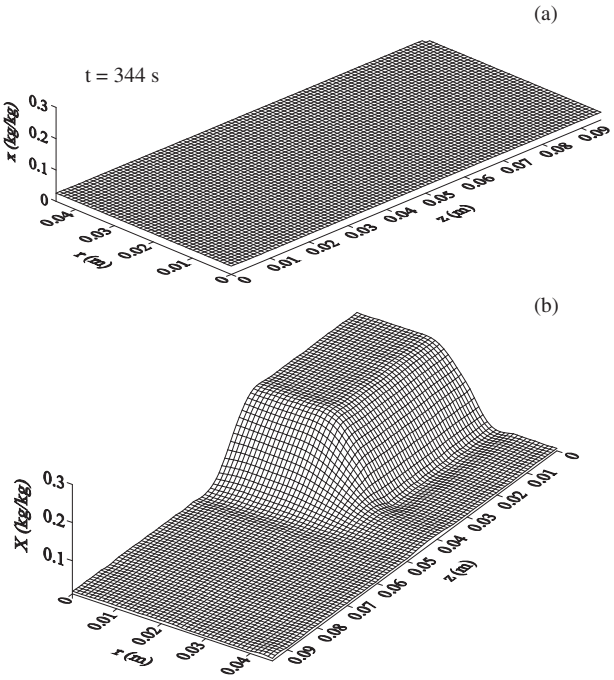

Figure 11. Comparison of time-space evolution of moisture content for 1D (a) and 2D (b) models: d = 10 mm, T_g = 140 °C and V_g = 1.5 m s^{-1}

evaporation rate leads to an increase of bed temperature. Consequently, the moisture content decreases. At the beginning, we note that the bed temperature is more important near the cylinder inlet and the wall in regard to its value at the cylinder middle (Figure 12). This is due to the drying agent (superheated steam) effects. In fact, superheated steam temperature is greater than that of the granular medium. Moreover, this temperature increase can be attributed to the wall heat flux application. Next the temperature decreases from the cylinder inlet to the outlet and from the wall to the center. Figure 11 presents the time-space evolution of the bed moisture content. In fact, the front movement follows the drying fluid blowing direction. Therefore the drying front moves from $Z = H$ to $Z = 0$.

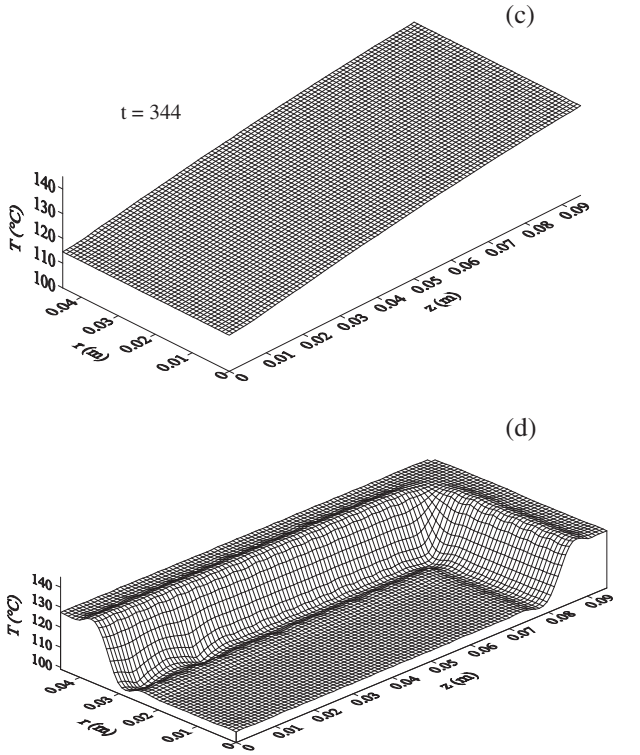

Figure 12. Comparison of time-space evolution of bed temperature for 1D (a) and 2D (b) models: d = 10 mm, T_g = 140 °C and V_g = 1.5 m s^{-1}.

Conclusion

A comprehensive heat and mass transfer model was developed for a packed bed drying process with superheated steam as drying agent. This model is based on the averaging volume approach. Taking into account the non validity of the thermal equilibrium hypothesis, a two temperatures model is presented: particle temperature (solid phase) and the gas temperature. The mass transfer is introduced by drying kinetics deduced from the particle model. The correlations of mass flux and moisture content, deduced from the numerical resolution of the single particle model, were incorporated in the bed model. The predicted results compared to the experimental data, indicated good agreements despite few discrepancies. The constructed numerical tool enabled us to predict the time-space variations of the bed temperature and the moisture content. We have also compared 1D and 2D models. Results show that the 2D model is more realistic. Indeed, time-space evolution of temperature and moisture content illustrates the existence of drying front for 2D model.

References

1. Thompson TL. 1970. Simulation for optimal grain dryer design. Transaction of the ASAE, 1(10), 844–848.
2. Riede Th, Schlünder EU. 1991. Selective through-drying in fixed beds. Chemical Engineering and Processing: Process Intensification, 29, 9–26.

3. Saastamoinen J, Impola R. 1997. Drying of biomass particles in fixed and moving beds. Drying Technology – International Journal, 5, 1919–1929.
4. Khan JA, Beasley DE, Alatas B. 1991. Evaporation from a packed bed of porous particles into superheated vapor. International Journal of Heat and Mass Transfer, 1, 267–280.
5. Hager J, Wimmerstedt R, Whitaker S. 2000. Steam drying a bed of porous spheres: theory and experiment. Chemical Engineering Science, 55, 1675–1698.
6. Chen Z, Agarwal PK, Agnew JB. 2001. Steam drying of coal, Part 2. Modeling the operation of fluidized bed drying unit. Fuel, 80, 209–223.
7. Tang Z, Cenkowski S, Muir WE. 2004. Modeling the superheated-steam drying of a fixed bed of brewers' spent grain. Biosystems Engineering, 87, 67–77.
8. Arnaud G, Fohr JP. 1988. Slow drying simulation in thick layers of granular products. International Journal of Heat and Mass Transfer, 31, 2517–2526.
9. Sözen M, Vafai K. 1990. Analysis of the nonthermal equilibrium condensing flow of gas through a packed bed. International Journal of Heat and Mass Transfer, 33, 1247–1261.
10. Mhimid A, Fohr JP, Ben Nasrallah S. 1999. Heat and mass transfer during drying of granular products by combined convection and conduction. Drying Technology – International Journal, 17, 1043–1063.
11. Ratti C, Mujumdar AS. 1995. Simulation of packed bed drying of foodstuffs with airflow reversal. Journal of Food Engineering, 26, 259–271.
12. Wang ZH, Chen G. 1999. Heat and mass transfer in fixed-bed drying. Chemical Engineering Science, 54, 4233–4243.
13. Kato K, Ohmura S, Taneda D, Onozawa I, Shimura K, Iijima A. 1981. Drying characteristics in a packed fluidized bed dryer. Journal Chemical Engineering Japan, 14, 365–371.
14. Izadifar M, Baik O-D, Simonson CJ. 2006. Modeling of the packed bed drying of paddy rice using the local volume averaging (LVA) approach. Food Research International, 39(6), 712–720.
15. Stakić M, Banjac M, Urošević T. 2011. Numerical study on hygroscopic material drying in packed bed. Brazilian Journal of Chemical Engineering, 28(2), 273–284.
16. Zili L, Ben Nasrallah S. 1999. Heat and mass transfer during drying in cylindrical packed beds. Numerical Heat Transfer, Part A, 36, 201.
17. Sitompul JP, Istadi I, Widiasa IN. 2001. Modeling and simulation of deep-bed grain dryers. Drying Technology – International Journal, 19(2), 269–280.
18. Istadi I, Sitompul JP. 2002. A comprehensive mathematical and numerical modeling of deep-bed grain drying. Drying Technology International Journal, 20(6), 1123–1142.
19. Sitompul JP, Istadi I, Sumardiono S. 2003. Modeling and simulation of momentum, heat and mass transfer in a deep-bed grain dryers. Drying Technology – International Journal, 21(2), 217–229.
20. Boukadida N, Ben Nasrallah S, Perre P. 2000. Mechanism of two-dimensional heat and mass transfer during convective drying of porous media under different drying conditions. Drying Technology : An International Journal, 18, 1367–1388.
21. Kumar P, Mujumdar AS. 1990. Superheated steam drying: a bibliography. Drying Technology – International Journal, 8(1), 195–205.
22. Pronyk C, Cenkowski S. 2003. Superheated steam drying technology. Paper number RRV03-0014, an ASAE Meeting Presentation.
23. Devahastin S, Suvarnakuta P, Soponronnarit S, Mujumdar AS. 2004. A comparative study of low-pressure superheated steam and vacuum drying of a heat-sensitive material. Drying Technology – International Journal, 22(8), 1845–1867.
24. Iyota H, Nishimura N, Onuma T, Nomura T. 2001. Drying of sliced raw potatoes in superheated steam and hot air. Drying Technology – International Journal, 19, 1411–1424.
25. Whitaker S. 1999. The Method of Volume Averaging. Kluwer: Dordrecht, The Netherlands.
26. Whitaker S. 1984. Moisture Transport mechanisms during the drying of granular porous media. Proceeding of the Fourth International Drying Symposium. Edited by Mujumdar AS, p. 31–42.
27. Whitaker S. 1991. Improved constraints for the principle of local thermal equilibrium. Industrial and Engineering Chemistry Research, 30, 983–997.
28. Hager J, Wimmerstedt R, Whitaker S. 2000. Steam drying a bed of porous spheres: theory and experiment. Chemical Engineering Science, 55, 1675.
29. Messai S, Sghaier J, Lecomte D, Belghith A. 2007. Drying kinetics of porous spherical particle and the inversion temperature. Drying Technology – International Journal, 26, 157.
30. Sghaier J, Jomaa W, Belghith A. 2008. Superheated steam of a spherical porous particle. Journal of Porous Media, 11, 633–646.
31. Patankar SV. 1980. Numerical Heat Transfer and Fluid Flow. Hemisphere Publishing Corporation, Mc Graw Hill: Washington.
32. Moyne C, Stemmelen D, Degiovanni A. 1990. Asymmetric drying of porous materials at high temperature: theoretical analysis and experiments. International Journal of Chemical Engineering, 30, 654.
33. Elustondo DM, Mujumdar AS, Urbicain MJ. 2002. Optimum operating conditions in drying foodstuffs with superheated steam. Drying Technology – International Journal, 20(2), 381–402.

Cite this article as: Messai S, El Ganaoui M, Sghaier J, Chrusciel L & Gabsi S: Comparison of 1D and 2D models predicting a packed bed drying. Int. J. Simul. Multisci. Des. Optim., 2014, **5**, A14.